Joint DOD and DOA Estimation for Bistatic MIMO Radar: A Covariance Trilinear Decomposition Perspective

FANGQING WEN[1,2], **(Member, IEEE), ZIJING ZHANG**[3]**, (Member, IEEE), AND GONG ZHANG**[4]**, (Member, IEEE)**

[1]National Demonstration Center for Experimental Electrical & Electronic Education, Yangtze University, Jingzhou 434023, China
[2]State Key Laboratory of Marine Resource Utilization in South China Sea, Hainan University, Haikou 570228, China
[3]National Laboratory of Radar Signal Processing, Xidian University, Xi'an 710071, China
[4]Key Laboratory of Radar Imaging and Microwave Photonics, Nanjing University of Aeronautics and Astronautics, Ministry of Education, Nanjing 210016, China

Corresponding author: Zijing Zhang (zjzhang@xidian.edu.cn)

ABSTRACT The covariance methods exert an effect on spatially colored (correlated) noise elimination during direction finding in multiple-input multiple-output (MIMO) radar. However, most of the existing methods seem difficulty to achieve a good balance between accuracy and efficiency. This paper aims at formulating a covariance trilinear decomposition perspective for direction-of-departure (DOD) and direction-of-arrival (DOA) estimation for bistatic MIMO radar. First, the array covariance matrix model is presented for de-noising. Furthermore, the noiseless covariance matrix is rearranged into a trilinear decomposition model. Finally, joint DOD and DOA estimation are linked to trilinear decomposition, which can be easily accomplished by exploiting the existing COMFAC technique. The proposed scheme can exploit the tensor structure of the covariance matrix, and it is attractive from the perspective of computational complexity. Moreover, it can be easily extended to the spatially colored noise scenario. The proposed algorithm is analyzed in terms of identifiability, flexibility, and complexity, and the stochastic Cramér-Rao bound on joint DOD and DOA estimation is derived. The computer simulations verify the effectiveness and improvement of the proposed method.

INDEX TERMS Array signal processing, bistatic MIMO radar, direction finding, spatially colored noise.

I. INTRODUCTION

Over the past decade, signal processing in multiple-input multiple-output (MIMO) radar has aroused a renewed attention. MIMO radar is characterized by the integrated of MIMO technique and radar detection. It simultaneously emits mutually orthogonal waveforms to illuminate the areas of interest, and try to capture the targets from the echoes received by multiple antennas [1]. Owing to the waveform diversity, MIMO radar is significantly superior to the traditional phased-array radar in terms of jamming and interference suppression, fading effect overcoming [2], [3], parameter estimation enhancement, et al. Usually, the MIMO radar system can be divided into statistical MIMO radar and colocated

MIMO radar according to its antenna geometry. The former utilize widely separated antenna to combat radar cross section (RCS) scintillation [4], while the latter exploit closely spaced antenna to obtain unambiguous angle estimation [5]. In this paper, we focus on the bistatic MIMO radar, which belongs to the latter.

Joint direction-of-departure (DOD) and direction-of-arrival (DOA) is a fundamental task in bistatic MIMO radar. Many efforts have been devoted and various algorithms have been proposed. Typical algorithm include spectrum grid search methods (e.g., Capon [6], [7], MUSIC [8]), propagator method (PM) [9], estimation of signal parameters via rotational invariance techniques (ESPRIT) [10], and optimization-based methods [11], [12]. Among which the spectrum grid search methods and the optimization-based methods are often computationally inefficient due to

exhaustive peak search. ESPRIT has attached a significant interest as it can obtain closed-form solution for direction estimation. PM can relief the calculation burden since it does not involve eigen-decomposition. Theoretically, the above mentioned methods can be summarized as matrix-based estimator, in which the array measurement is arranged into a matrix, and the multi-dimensional structure inherent in the matched array measurement has been ignored. Unlike matrix-based methods, tensor-based estimators are powerful to exploit the strong algebraic structure [13], thus they usually provide more accurate estimation performance. Two tensor models are widely used in tensor algebraic, named Tucker tensor and Kruskal Tensor [14]. Accordingly, two main strategies, termed higher-order singular value decomposition (HOSVD) and parallel factor (PARAFAC) analysis [15], [16], are utilized for tensor decomposition,. The HOSVD is the higher-order analogue of singular value decomposition (SVD), which tries to find a set of basis for each tensor unfolding. The PARAFAC method factorizes a tensor into a sum of rank-one tensors. Some tensor-based approaches have been introduced in [17]–[20]. In [17], a direct HOSVD method and a covariance HOSVD (C-HOSVD) method are proposed, which turn out to be effect to achieve more accurate subspaces estimation. A real-valued version is proposed in [21], which relief the calculation burden of the HOSVD method. The PARAFAC estimator is introduced in [18] followed by an improved version with larger virtual aperture [19] and a real-valued variant [20]. Also, many efforts have been tried in robust direction finding with array imperfections [22]–[25]. Usually, the HOSVD is directly computed via multiple truncated SVDs, while the PARAFAC decomposition is accomplished via alternative least squares (ALS) algorithm. In contrast, the PARAFAC estimator is more accurate but less efficient, since the ALS is sensitive to the initialization.

Unfortunately, as suggested in the literature, the aforementioned tensor estimators are only effective with Gaussian white noise. In the presence of spatially colored (correlated) noise, their performance would degrade or even fail to work. Several improved algorithms have been proposed to deal with the colored noise in bistatic MIMO radar. In [26]–[29], the spatial cross-correlation methods has been proposed, in which the transmit array in these methods is divided into several subarrays, the non-correlation characteristic of the matched noise associated with different transmit antenna is explored. Assume that the noise associated with various pulse are uncorrelated, the temporal cross-correlation algorithms have been derived in [30]–[32]. In these algorithms, the array measurement is divided into two groups according to the temporal index, the cross-correlation of the above two groups is exploited to suppress the spatial colored noise. Additionally, suppose that the noise field is invariant under two measurements of the array covariance, the effect of the spatial colored noise can be removed through covariance differencing [33], [34]. Comparatively speaking, the spatial cross correlation approaches are suffering from

the virtual aperture loss, since the dimension of the covariance matrix is reduced. Although the covariance differencing algorithms can exploit the full DOF of the virtual aperture of the MIMO radar, they are less efficient than the temporal cross-correlation methods, since additional calculation is required in determining the unambiguous directions. It should be emphasized all these de-noising methods are relay on the array covariance (or cross-covariance). Moreover, as shown in the literature, the PARAFAC variant offer more accurate performance than the HOSVD version [32], since the former utilizes more degree-of-freedom (DOF). Nevertheless, the fourth-order PARAFAC estimator is quit sensitive to the initializations and may suffers from the slowness of the convergence steps, making it unsuitable for massive MIMO configuration [35], [36].

In this paper, we revisit the DOD and DOA estimation problem in bistatic MIMO radar, and a covariance-based trilinear decomposition estimator is proposed. The contributions of this paper are listed as follows:

(a). The covariance-PARAFAC model is established. By rearranging the covariance matrix into a fourth-order tensor, the proposed PARAFAC model is able to capture the multidimensional structure of the covariance measurement.

(b). A fast implication scheme is proposed. By exploiting the low-rank property as well as the multidimensional structure of the cross-covariance measurement, an innovative third-order PARAFAC (trilinear decomposition) model is formulated, thus the PARAFAC decomposition of the covariance tensor can be accomplished via the existing COMFAC algorithm. In contrast to the state-of-the-art quadrilinear least squares (QALS) approach, the proposed estimator can be quickly implemented.

(c). We illustrate how does the proposed estimator extended to the spatially colored noise scenario. Actually, the proposed estimator can be easily combined with the existing de-noising strategies. Herein, the existing temporal cross-correlation strategy is utilized as an example.

(d). The proposed estimator is analyzed in terms of identifiability, flexibility, complexity as well as stochastic Cramér-Rao bound (CRB). The advantages of the proposed estimator are verified by numerical simulations.

This paper is organized as follows. The data model for DOD and DOA estimaiton in bistatic MIMO radar is elaborated in section II. The proposed covariance-trilinear decomposition estimator is given in section III. Detailed analysis are described in section IV. Numerical simulations and discussions are presented in section V. Finally, a brief conclusion is provided in section VI.

II. TENSOR PRELIMINARIES SIGNAL MODEL

A tensor is the higher-order analogue of a vector and a matrix [32]. Before given the details of the proposed algorithm, let us first introduce some necessary preliminaries concerning tensor, which can be find in our pervious work [32].

Definition 1(Unfolding): The mode-n unfolding of an N-th order tensor $\mathcal{X}$ is denoted by $[\mathcal{X}]_{(n)}$.

The $(i_1, i_2, \cdots, i_N)$-element of $\mathcal{X}$ maps to the (i_n, j)-th element of $[\mathcal{X}]_{(n)}$, where $j = 1 + \sum_{k=1, k \neq n}^{N} (i_k - 1) J_k$ with $J_k = \prod_{m=1, m \neq n}^{k-1} I_m$.

Definition 2 (Mode-n Tensor-Matrix Product): The mode-n product of an N-order tensor $\mathcal{X} \in \mathbb{C}^{I_1 \times I_2 \times \cdots \times I_N}$ and a matrix $\mathbf{A} \in \mathbb{C}^{J_n \times I_n}$, denoted by $\mathcal{X} \times_n \mathbf{A}$, is a tensor of size $I_1 \times \cdots \times I_{n-1} \times J_n \times I_{n+1} \times \cdots \times I_N$, obtained by taking the inner product between each mode-n fiber and the rows of the matrix $\mathbf{A}$, i.e.,

$$\mathcal{Y} = \mathcal{X} \times_n \mathbf{A} \iff [\mathcal{Y}]_{(n)} = \mathbf{A} [\mathcal{X}]_{(n)} \tag{1}$$

Definition 3 (PARAFAC Decomposition): The PARAFAC decomposition of an N-order tensor $\mathcal{X}$ with rank-K is given by

$$\mathcal{X} = \sum_{k=1}^{K} g_k \mathbf{a}_k^{(1)} \circ \mathbf{a}_k^{(2)} \circ \cdots \circ \mathbf{a}_k^{(N)} \tag{2}$$

where $\mathbf{a}_k^{(n)} \in \mathbb{C}^{I_n \times 1}$, $\circ$ denotes the outer product. Obviously, the PARAFAC decomposition expresses $\mathcal{X}$ into a sum of K rank one tensors. In mode-n tensor-matrix product form, (2) can be expressed as

$$\mathcal{X} = \mathcal{G} \times_1 \mathbf{A}^{(1)} \times_2 \mathbf{A}^{(2)} \cdots \mathbf{A}^{(N-1)} \times_N \mathbf{A}^{(N)} \tag{3}$$

where $\mathcal{G} \in \mathbb{C}^{K \times K \times \cdots \times K}$ is a 'diagonal' tensor with the $(k, k, \cdots, k)$-th element is g_k and zeros elsewhere. $\mathbf{A}^{(n)} = \left[\mathbf{a}_1^{(n)}, \mathbf{a}_2^{(n)}, \cdots, \mathbf{a}_K^{(n)} \right] \in \mathbb{C}^{I_n \times K}$, $n = 1, 2, \cdots N$. Also, $\mathcal{X}$ can be rearranged in matrix style as

$$[\mathcal{X}]_{(n)} = \mathbf{A}^{(n)} \mathbf{G} \left[\mathbf{A}^{(n+1)} \odot \mathbf{A}^{(n+2)} \odot \cdots \mathbf{A}^{(N)} \odot \right.$$
$$\left. \mathbf{A}^{(1)} \odot \mathbf{A}^{(2)} \cdots \odot \mathbf{A}^{(n-1)} \right]^T \tag{4}$$

where $\mathbf{G} = \text{diag} \{[g_1, g_2, \cdots, g_K]\}$, the superscript $(\cdot)^T$ represents transpose, $\odot$ denotes the KhatriRao product.

Definition 4: (Generalized Tensorization of a PARAFAC model [37]): For the PARAFAC decomposition model in (2), let the order sets $\mathbb{O}_j = \left\{ o_{j,1}, o_{j,2}, \cdots, o_{j,M_j} \right\}$ for $j = 1, 2, \cdots, J$ be a partitioning of the dimensions $\mathbb{O} = \{1, 2, \cdots, N\}$, the generalized tensorization of $\mathcal{X}$ is denoted by a new tensor $\mathcal{X}_{\mathbb{O}_1, \mathbb{O}_2, \cdots, \mathbb{O}_J} \in \mathbb{C}^{T_1 \times T_2 \times \cdots \times T_J}$ with

$$\mathcal{X}_{\mathbb{O}_1, \mathbb{O}_2, \cdots, \mathbb{O}_J} = \sum_{k=1}^{K} g_k \mathbf{b}_k^{(1)} \circ \mathbf{b}_k^{(2)} \circ \cdots \circ \mathbf{b}_k^{(J)} \tag{5}$$

where $T_j = \prod_{m=1}^{M_j} I_{o_{j,m}}$, $\mathbf{b}_k^{(j)} = \mathbf{a}_k^{\left(o_{j,M_j}\right)} \otimes \mathbf{a}_k^{\left(o_{j,M_j-1}\right)} \cdots, \otimes \mathbf{a}_k^{(o_{j,1})}$, $\otimes$ stands for the Kronecker product. The above definition can be easily obtained by exploiting the unfolding of $\mathcal{X}$.

As shown in Figure 1, we consider a bistatic MIMO radar system (the transmit antennas and the receive antennas are in the far-field of each other) with an M-element transmit array and an N-element receive array. Assume that there are K slow moving targets appear in the far-field (within the same range bin), and the DOD-DOA-Doppler frequency pair for the k-th
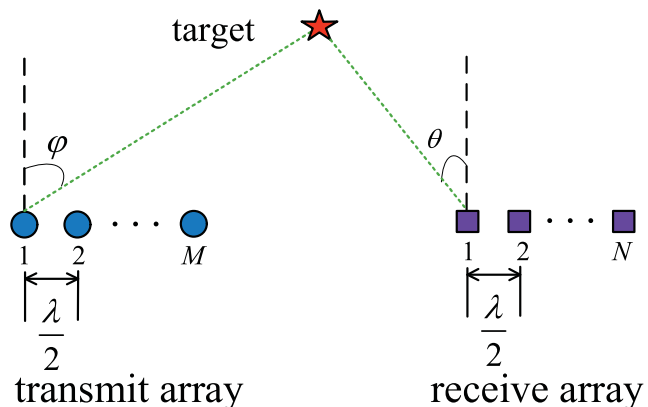

FIGURE 1. Illustration of bistatic MIMO radar [32].

target is $(\varphi_k, \theta_k, f_k)$. Suppose that the transmit elements emit orthogonal narrowband pulse waveforms $\{s_m (t)\}_{m=1}^{M}$, i.e.,

$$\int_{T_p} s_m (t) s_n^* (t) \, dt = \delta (m - n) \tag{6}$$

where t is the fast time index, T_p denotes the pulse duration, the superscript $(\cdot)^*$ represents conjugate and $\delta (\cdot)$ is the Kronecker delta. The echo from the k-th target is modeled as [38]

$$r_k (t, \tau) = b_k (\tau) \mathbf{a}_t^T (\varphi_k) \mathbf{s} (t) \tag{7}$$

where $b_k (\tau) = \beta_{k,\tau} e^{j2\pi f_k \tau}$, τ is the slow time (pulse) index, $\beta_{k,\tau}$ is the reflection amplitude of the k-th target during the τ-th pulse duration, $\mathbf{a}_t (\varphi_k) \in \mathbb{C}^{M \times 1}$ represents the corresponding transmit steering vector, $\mathbf{s} (t) = [s_1 (t), s_2 (t), \cdots, s_M (t)]^T$ is the transmit waveform vector. The noisy observation at the receiver is then given by

$$\mathbf{x} (t, \tau) = \sum_{k=1}^{K} b_k (\tau) \mathbf{a}_r (\theta_k) \mathbf{a}_t^T (\varphi_k) \mathbf{s} (t) + \mathbf{w} (t, \tau) \tag{8}$$

where $\mathbf{a}_r (\theta_k) \in \mathbb{C}^{N \times 1}$ is the receive steering vector corresponding to the k-th target, $\mathbf{w} (t, \tau)$ is the additive noise vector. Before the detailed derivation, the following assumptions are made:

A1. The transmit array and the receive array are linear arrays, and they have been well calibrated, i.e., sensor errors (e.g., gain-phase error, mutual coupling) are beyond the scope of this paper.

A2. $\{\theta_k\}_{k=1}^{K}$ are distinct with each other, and so as to $\{\varphi_k\}_{k=1}^{K}$ and $\{f_k\}_{k=1}^{K}$.

A3. The targets are uncorrelated, i.e., $\text{E} \left\{ b_{k1} (\tau) b_{k2}^* (\tau) \right\} = \begin{cases} 0, & k1 \neq k2 \\ \alpha_k, & k1 = k2 = k \end{cases}$, where α_k is the power of the k-th target reflection coefficient, $\text{E} \{\cdot\}$ returns the expectation of a variable.

A4. The noise vector $\mathbf{w} (t, \tau)$ is temporally Gaussian white, spatially correlated, i.e., $\text{E} \left\{ \mathbf{w} (t_1, \tau) \mathbf{w}^H (t_2, \tau) \right\} = \mathbf{C} \cdot \delta (t_1 - t_2)$, the superscript $(\cdot)^H$ denotes Hermitian transpose.

Matching $\mathbf{x}(t, \tau)$ with $s_m(t)$ yields

$$
\begin{aligned}
\mathbf{y}_m(\tau) &= \int_{T_p} \mathbf{x}(t, \tau) s_m^*(t) dt \\
&= \sum_{k=1}^{K} b_k(\tau) \mathbf{a}_r(\theta_k) \mathbf{a}_t^T(\varphi_k) \int_{T_p} \mathbf{s}(t) s_m^*(t) dt \\
&\quad + \int_{T_p} \mathbf{w}(t, \tau) s_m^*(t) dt \\
&= \sum_{k=1}^{K} b_k(\tau) a_t^m(\varphi_k) \mathbf{a}_r(\theta_k) + \mathbf{n}_m(\tau)
\end{aligned} \tag{9}
$$

where $a_t^m(\varphi_k)$ denotes the m-th entity of $\mathbf{a}_t(\varphi_k)$, $\mathbf{n}_m(\tau) = \int_{T_p} \mathbf{w}(t, \tau) s_m^*(t) dt$. By arranging all the outputs as $\mathbf{y}(\tau) = \left[\mathbf{y}_1^T(\tau), \mathbf{y}_2^T(\tau), \cdots, \mathbf{y}_M^T(\tau)\right]$, we can get

$$
\begin{aligned}
\mathbf{y}(\tau) &= \sum_{k=1}^{K} [\mathbf{a}_t(\varphi_k) \otimes \mathbf{a}_r(\theta_k)] b_k(\tau) + \mathbf{n}(\tau) \\
&= [\mathbf{A}_t \odot \mathbf{A}_r] \mathbf{b}(\tau) + \mathbf{n}(\tau)
\end{aligned} \tag{10}
$$

where $\mathbf{n}(\tau) = \left[\mathbf{n}_1^T(\tau), \mathbf{n}_2^T(\tau), \cdots, \mathbf{n}_M^T(\tau)\right]^T$, $\mathbf{b}(\tau) = [b_1(\tau), b_2(\tau), \cdots, b_K(\tau)]^T$, $\mathbf{A}_t = [\mathbf{a}_t(\varphi_1), \mathbf{a}_t(\varphi_2), \cdots, \mathbf{a}_t(\varphi_K)] \in \mathbb{C}^{M \times K}$ and $\mathbf{A}_r = [\mathbf{a}_r(\theta_1), \mathbf{a}_r(\theta_2), \cdots, \mathbf{a}_r(\theta_K)] \in \mathbb{C}^{N \times K}$ are, respectively, the transmit direction matrix and the receive direction matrix. Accordingly, the covariance matrix of $\mathbf{y}(\tau)$ is

$$
\begin{aligned}
\mathbf{R}_y &= \mathrm{E}\left\{\mathbf{y}(\tau) \mathbf{y}^H(\tau)\right\} \\
&= \mathbf{A} \mathbf{R}_b \mathbf{A}^H + \mathbf{R}_n \\
&= \mathbf{R}_s + \mathbf{R}_n
\end{aligned} \tag{11}
$$

where $\mathbf{A} = \mathbf{A}_t \odot \mathbf{A}_r$ denotes the virtual direction matrix, $\mathbf{R}_b = \mathrm{diag}\{[\alpha_1, \alpha_2, \cdots, \alpha_K]\}$ represents the target covariance matrix, where $\mathrm{diag}\{\mathbf{r}\}$ denotes the diagonalization operation. $\mathbf{R}_s = \mathbf{A} \mathbf{R}_b \mathbf{A}^H$ and $\mathbf{R}_n = \mathrm{E}\left\{\mathbf{n}(\tau) \mathbf{n}^H(\tau)\right\}$, respectively, denote the signal covariance matrix and the noise covariance matrix. It is easily to find that $\mathbf{R}_s$ is a low-rank noise-free matrix. Now we focus on $\mathbf{R}_n$. It is follows that $\mathbf{n}(\tau) = \int_{T_p} \mathbf{s}^*(t) \otimes \mathbf{w}(t, \tau) dt$, and hence

$$
\begin{aligned}
\mathbf{R}_n &= \mathrm{E}\left\{\int_{T_p} \int_{T_p} [\mathbf{s}^*(t_1) \otimes \mathbf{w}(t_1, \tau)]\right. \\
&\quad \left. \cdot \left[\mathbf{s}^T(t_2) \otimes \mathbf{w}^H(t_2, \tau)\right] dt_1 dt_2\right\} \\
&= \int_{T_p} \int_{T_p} \mathrm{E}\left\{\mathbf{s}^*(t_1) \mathbf{s}^T(t_2)\right\} \otimes \mathrm{E}\left\{\mathbf{w}(t_1, \tau) \mathbf{w}(t_2, \tau)\right\} dt_1 dt_2 \\
&= \int_{T_p} \int_{T_p} \left[\mathbf{s}(t_1) \mathbf{s}^H(t_2)\right]^* \otimes [\mathbf{C} \cdot \delta(t_1 - t_2)] dt_1 dt_2 \\
&= \mathbf{I}_M \otimes \mathbf{C}
\end{aligned} \tag{12}
$$

where $\mathbf{I}_M$ denotes the $M \times M$ identity matrix, and the property in (6), assumption **A4** as well as the property $(\mathbf{A}_1 \otimes \mathbf{A}_2)(\mathbf{A}_3 \otimes \mathbf{A}_4) = (\mathbf{A}_1 \mathbf{A}_3) \otimes (\mathbf{A}_2 \mathbf{A}_4)$ are utilized in the derivation.

In practice, $\mathbf{y}(\tau)$ is sampled at instances $\tau = 1/f_s, 2/f_s, \cdots, L/f_s$, and L snapshots $\mathbf{Y} = [\mathbf{y}(1/f_s), \mathbf{y}(2/f_s), \cdots, \mathbf{y}(L/f_s)] \in \mathbb{C}^{MN \times L}$ are collected. Consequently, (10) is replaced by

$$
\mathbf{Y}_s = [\mathbf{A}_t \odot \mathbf{A}_r] \mathbf{B}_f^T + \mathbf{N}_s \tag{13}
$$

where $\mathbf{B}_f = [\mathbf{b}(f_1), \mathbf{b}(f_2), \cdots, \mathbf{b}(f_K)] \in \mathbb{C}^{L \times K}$ denotes the characteristic matrix of the target, $\mathbf{b}(f_k) = \left[\beta_{k,1} e^{j2\pi f_k/f_s}, \beta_{k,2} e^{j4\pi f_k/f_s}, \cdots, \beta_{k,L} e^{j2L\pi f_k/f_s}\right]^T$ is the k-th column of $\mathbf{B}_f$. $\mathbf{N}_s = [\mathbf{n}(1/f_s), \mathbf{n}(2/f_s), \cdots, \mathbf{n}(L/f_s)] \in \mathbb{C}^{MN \times L}$ stands for the observation of the matched noise. Also, $\mathbf{R}_y$ is estimated via

$$
\hat{\mathbf{R}}_y = \frac{1}{L} \sum_{l=1}^{L} \mathbf{y}_l \mathbf{y}_l^H \tag{14}
$$

According to assumption **A2**, the matrices $\mathbf{A}_t$, $\mathbf{A}_r$ and $\mathbf{B}_f$ are rank-K. Therefore, the model in (13) can be interpreted as a third-order noisy PARAFAC model as

$$
\begin{aligned}
\mathcal{Y} &= \sum_{k=1}^{K} \mathbf{a}_t(\varphi_k) \circ \mathbf{a}_r(\theta_k) \circ \mathbf{b}(f_k) + \mathcal{N} \\
&= \mathcal{I}_{3,K} \times_1 \mathbf{A}_t \times_2 \mathbf{A}_r \times_3 \mathbf{B}_f + \mathcal{N}
\end{aligned} \tag{15}
$$

where $\mathcal{I}_{3,K}$ is a $K \times K \times K$ identity tensor, i.e., the (k, k, k)-th $(k = 1, 2, \cdots, K)$ element is one, and zero elsewhere. Also, (14) is known as the trilinear decomposition model. It is easy to find the relation between (13) and (34)

$$
\begin{cases} \mathbf{Y}_s = [\mathcal{Y}]_{(3)}^T \\ \mathbf{N}_s = [\mathcal{N}]_{(3)}^T \end{cases} \tag{16}
$$

III. THE PROPOSED ALGORITHM
A. WHITE NOISE SCENARIO
When the received array noise is spatially white, $\mathbf{C} = \sigma^2 \mathbf{I}_N$ and $\mathbf{R}_n = \sigma^2 \mathbf{I}_{MN}$, where σ^2 is the power of the noise. Usually, eigendecomposition is performed on $\mathbf{Y}$, or alternatively, on $\hat{\mathbf{R}}_y$ to obtain the subspaces. With the intention of utilizing the multidimensional nature inherit in $\mathbf{Y}$, the direct trilinear decomposition algorithm is proposed in [18], which tries to optimize

$$
\min_{\mathbf{A}_t, \mathbf{A}_r, \mathbf{B}} \left\| \mathcal{Y} - \mathcal{I}_{3,K} \times_1 \mathbf{A}_t \times_2 \mathbf{A}_r \times_3 \mathbf{B} \right\|_F \tag{17}
$$

$\|\cdot\|_F$ accounts for the Frobenius norm. The above problem is resolved via the trilinear ALS technique, which fixes two factor matrices and fits the residual one alternatively until convergence conditions have been stratified, ie.,

$$
\begin{cases} \min_{\mathbf{B}_f} \left\| \mathbf{Y}_s - [\mathbf{A}_t \odot \mathbf{A}_r] \mathbf{B}_f^T \right\|_F \\ \min_{\mathbf{A}_t} \left\| \mathbf{Y}_t - [\mathbf{A}_r \odot \mathbf{B}_f] \mathbf{A}_t^T \right\|_F \\ \min_{\mathbf{A}_r} \left\| \mathbf{Y}_r - [\mathbf{B}_f \odot \mathbf{A}_t] \mathbf{A}_r^T \right\|_F \end{cases} \tag{18}
$$

where $\mathbf{Y}_t = [\mathcal{Y}]_{(1)}^T$, $\mathbf{Y}_r = [\mathcal{Y}]_{(2)}^T$. Trilinear ALS is quite easy to implement and is guaranteed to converge [22]. However, ALS suffers from the slowness of the convergence steps [39],

since it is very sensitive to the initialization. In this paper, the computationally efficient COMFAC algorithm in [40] is utilized. In COMFAC, the third-order tensor is first compressed via the Tucker algorithm. Thereafter, the fitting operations are conducted in the condensed space, which only require a few TALS steps. Finally, the solutions are recovered to the original space by using the Tucker loadings [24].

Similar to (14), the low-rank signal covariance matrix $\mathbf{R}_s$ can be written in tensor format as [32]

$$\mathcal{R}_s = \sum_{k=1}^{K} \alpha_k \mathbf{a}_t (\varphi_k) \circ \mathbf{a}_r (\theta_k) \circ \mathbf{a}_t^* (\varphi_k) \circ \mathbf{a}_r^* (\theta_k)$$
$$= \mathcal{R}_{b} \times_1 \mathbf{A}_t \times_2 \mathbf{A}_r \times_3 \mathbf{A}_t^* \times_4 \mathbf{A}_r^* \quad (19)$$

where $\mathcal{R}_{b} \in \mathbb{C}^{K \times K \times K \times K}$ is a fourth-order tensor with the (k, k, k, k)-th $(k = 1, 2, \cdots, K)$ element equals to α_k and zeros elsewhere. Actually, $\mathbf{R}_y$ considered as a multi-mode unfolding of $\mathcal{R}_y$ [15], denoted as $\mathbf{R}_y = [\mathcal{R}_y]_{(\mathbf{H})}$. With sufficient snapshots, $\hat{\sigma}^2$, the estimation of σ^2, can be easily estimated via the matrix decomposition or the Tucker decomposition technique. Hence, $\mathbf{R}_s$ can be estimated via $\hat{\mathbf{R}}_s = \hat{\mathbf{R}}_y - \hat{\sigma}^2 \mathbf{I}_{MN}$. Estimating $\mathbf{A}_t$ and $\mathbf{A}_r$ is transferred into approximating

$$\min_{\mathbf{A}_t, \mathbf{A}_r, \mathbf{R}_b} \left\| \hat{\mathcal{R}}_s - \mathcal{R}_{b} \times_1 \mathbf{A}_t \times_2 \mathbf{A}_r \times_3 \mathbf{A}_t^* \times_4 \mathbf{A}_r^* \right\|_F \quad (20)$$

where $\hat{\mathbf{R}}_s = \left[\hat{\mathcal{R}}_s \right]_{(\mathbf{H})}$. A common solver to the above problem is QALS. Similar to TALS, QALS has very poor convergence. According to **Definition 4**, by defining $\mathbb{O}_1 = \{1\}$, $\mathbb{O}_2 = \{2\}$ and $\mathbb{O}_3 = \{3, 4\}$, $\mathcal{R}_s$ can be stacked into a third-order tensor $\mathcal{R}_{s,\text{new}}$ as

$$\mathcal{R}_{s,\text{new}} = \sum_{k=1}^{K} \mathbf{a}_t (\varphi_k) \circ \mathbf{a}_r (\theta_k) \circ \left(\alpha_k \mathbf{a}_{tr}^* (\theta_k, \varphi_k) \right)$$
$$= \mathcal{I}_{3,K} \times_1 \mathbf{A}_t \times_2 \mathbf{A}_r \times_3 \tilde{\mathbf{A}}^* \quad (21)$$

where $\mathbf{a}_{tr}^* (\theta_k, \varphi_k) = \mathbf{a}_t^* (\varphi_k) \otimes \mathbf{a}_r^* (\theta_k)$, $\tilde{\mathbf{A}} = \mathbf{A} \mathbf{R}_b$. Obviously, (21) gives the trilinear decomposition model of $\mathcal{R}_{s,\text{new}}$. By exploiting COMFAC algorithm on the estimate of $\mathcal{R}_{s,\text{new}}$, $\mathbf{A}_t$ and $\mathbf{A}_r$ can be easily estimated, which fulfills [16]

$$\begin{cases} \hat{\mathbf{A}}_t = \Pi \mathbf{A}_t \Delta_1 + \mathbf{N}_1 \\ \hat{\mathbf{A}}_r = \Pi \mathbf{A}_r \Delta_2 + \mathbf{N}_2 \end{cases} \quad (22)$$

where Π is a permutation matrix, $\mathbf{N}_1$ and $\mathbf{N}_2$ represent the corresponding fitting errors, Δ_1 and Δ_2 stand for the diagonal scaling matrices. Note that $\hat{\mathbf{A}}_t$ and $\hat{\mathbf{A}}_r$ are Vandermonde-like, the least squares (LS) method is suitable for joint DOD and DOA estimation. Define

$$\begin{cases} \mathbf{P}_t = \begin{bmatrix} 1 & 1 & \cdots & 1 \\ 0 & 2\pi d_{t,2}/\lambda & \cdots & 2\pi d_{t,M}/\lambda \end{bmatrix}^T \\ \mathbf{P}_r = \begin{bmatrix} 1 & 1 & \cdots & 1 \\ 0 & 2\pi d_{r,2}/\lambda & \cdots & 2\pi d_{r,N}/\lambda \end{bmatrix}^T \end{cases} \quad (23)$$

where $d_{t,m}$ is the distance between the m-th transmit element and the first transmit element, and $d_{r,n}$ is the distance between the n-th receive element and the first receive element, λ denotes the carrier wavelength. Let $\hat{\mathbf{a}}_t (\varphi_k)$ and $\hat{\mathbf{a}}_r (\theta_k)$ are the k-th column of $\hat{\mathbf{A}}_t$ and $\hat{\mathbf{A}}_r$, respectively. Denote $\begin{cases} \mathbf{h}_{tk} = -\text{phase} \left\{ \hat{\mathbf{a}}_t (\varphi_k) \right\} \\ \mathbf{h}_{rk} = -\text{phase} \left\{ \hat{\mathbf{a}}_r (\theta_k) \right\} \end{cases}$, where phase$\{\cdot\}$ is to get the phase. Then compute

$$\begin{cases} \mathbf{u}_k = \mathbf{P}_1^\dagger \mathbf{h}_{tk} \\ \mathbf{v}_k = \mathbf{P}_2^\dagger \mathbf{h}_{rk} \end{cases} \quad (24)$$

where the superscript $(\cdot)^\dagger$ denotes the pseudo-inverse. Notably, the second entity of $\mathbf{u}_k$ and $\mathbf{v}_k$, given by $u_{k,2}$ and $v_{k,2}$, respectively, contain the directions of the k-th target. The k-th DOD and DOA can be estimated via

$$\begin{cases} \hat{\varphi}_k = \arcsin(u_{k,2}) \\ \hat{\theta}_k = \arcsin(v_{k,2}) \end{cases} \quad (25)$$

It should be noted that $\hat{\mathbf{A}}_t$ and $\hat{\mathbf{A}}_r$ share the same permutation, hence the DODs and the DOAs are paired automatically.

B. SPATIALLY COLORED NOISE SCENARIO

In the presence of spatially colored noise, the traditional subspace-based algorithms may significantly degenerated. Moreover, approaches such as the direct PARAFAC decomposition method and the ML estimator could neither perform properly. Typical strategies to suppress the spatially colored noise are rely on the covariance output of the measurement [26]- [32]. Since the PARAFAC model in this paper is based on the covariance matrix of the samples, it can be easily extended to the colored noise scenario. Taking the temporal cross-correlation framework [30] as an example, we will illustrate the extension details. For any $\tau_1 - \tau_2 = \Delta \neq 0$, according to the **A3**, we have

$$\text{E} \left\{ \mathbf{w} (t, \tau_1) \mathbf{w}^H (t, \tau_2) \right\} = \mathbf{0} \quad (26)$$

which mean the spatially colored noise is temporal uncorrelated. Consequently, we can get

$$\mathbf{R}_{n1} = \text{E} \left\{ \mathbf{n} (\tau_1) \mathbf{n}^H (\tau_2) \right\}$$
$$= \int \int_{T_p} \left[\mathbf{s} (t_1) \mathbf{s}^H (t_2) \right]^*$$
$$\otimes \text{E} \left\{ \mathbf{w} (t_1, \tau_1) \mathbf{w}^H (t_2, \tau_2) \right\} dt_1 dt_2$$
$$= \mathbf{0} \quad (27)$$

which indicates the matched array noises associated with various pulses are uncorrelated. Besides, we have

$$\text{E} \left\{ b_k (\tau_1) b_k^* (\tau_2) \right\} = e^{j2\pi f_k \Delta} \cdot \text{E} \left\{ \beta_k (\tau_1) \beta_k (\tau_2) \right\} = \gamma_k \quad (28)$$

where γ_k is a nonzero constant. (28) reveals that the $\mathbf{b} (\tau)$ is temporal correlated. In combination with **A3**, we obtain

$$\text{E} \left\{ \mathbf{b} (\tau_1) \mathbf{b}^H (\tau_2) \right\} = \Gamma \quad (29)$$

where $\Gamma = \text{diag}\{\gamma_1, \gamma_2, \cdots, \gamma_K\}$. Furthermore, we have

$$\mathbf{R} = \mathrm{E}\left\{\mathbf{y}(\tau_1)\,\mathbf{y}^H(\tau_2)\right\} = \mathbf{A}\Gamma\mathbf{A}^H \qquad (30)$$

Obviously, the effect of the spatially colored noise is removed from the temporal cross-correlation of $\mathbf{y}(\tau)$. Let $\Delta = 1/f_s$, $\mathbf{R}$ can be estimated via

$$\hat{\mathbf{R}} = \frac{1}{L-1}\mathbf{Y}_1\mathbf{Y}_2^H \qquad (31)$$

where $\mathbf{Y}_1$ and $\mathbf{Y}_2$ consist of the first $L-1$ columns and the last $L-1$ columns of $\mathbf{Y}$, respectively. Similar to (21), $\mathbf{R}$ can be rearranged into a third-order PARAFAC decomposition model as

$$\mathcal{R} = \mathcal{I}_{3,K} \times_1 \mathbf{A}_t \times_2 \mathbf{A}_r \times_3 \bar{\mathbf{A}}^* \qquad (32)$$

where $\bar{\mathbf{A}}^* = \mathbf{A}\Gamma$. Utilizing the COMFAC algorithm to perform PARAFAC decomposition for $\mathcal{R}$, one can get the estimation of $\mathbf{A}_t$ and $\mathbf{A}_r$. With the LS method in the last subsection, the DODs and DOAs can be easily estimated. It should be noted that the temporal cross-correlation scheme is only suitable for scenario where $\mathbf{b}(\tau)$ is temporally correlated, e.g., the Doppler frequency of the targets is time invariant during L snapshots, otherwise it may fail to work.

C. ALGORITHM SUMMARIZATION
To help the reader to repeat the results of this paper, we summarize the algorithmic steps for the proposed estimators in Table 1 and Table 2.

TABLE 1. Algorithmic steps in white noise scenario.

Step	Operation
1	Estimate the array covariance matrix $\mathbf{R}_y$ via $\hat{\mathbf{R}}_y = \frac{1}{L}\sum_{l=1}^{L}\mathbf{y}_l\mathbf{y}_l^H$.
2	Obtain the signal covariance matrix $\mathbf{R}_s$ via $\hat{\mathbf{R}}_s = \hat{\mathbf{R}}_y - \hat{\sigma}^2\mathbf{I}_{MN}$, where $\hat{\sigma}^2$ is the estimated noise variance.
3	Arrange the signal covariance matrix into a fourth-order tensor $\hat{\mathcal{R}}_s$ that $\hat{\mathbf{R}}_s = \left[\hat{\mathcal{R}}_s\right]_{(\mathbf{H})}$. Furthermore, by defining $\mathbb{O}_1 = \{1\}$, $\mathbb{O}_2 = \{2\}$ and $\mathbb{O}_3 = \{3,4\}$, rearrange $\hat{\mathcal{R}}_s$ into a third order tensor $\mathcal{R}_{s,\text{new}}$ according to **Definition 4**.
4	Obtain trilinear decomposition of $\mathcal{R}_{s,\text{new}}$ via the COMFAC algorithm, thus obtain the estimates of $\mathbf{A}_t$ and $\mathbf{A}_r$.
5	Construct $\mathbf{P}_t$ and $\mathbf{P}_r$ according to Eq.(23), and then get the DODs and DOAs via Eq.(24) and Eq.(25).

TABLE 2. Algorithmic steps in spatially colored noise scenario.

Step	Operation
1	Estimate the noiseless array covariance matrix $\mathbf{R}$ via $\hat{\mathbf{R}} = \frac{1}{L-1}\mathbf{Y}_1\mathbf{Y}_2^H$.
2	Arrange $\hat{\mathbf{R}}$ into a third-order tensor $\hat{\mathcal{R}}$.
3	Obtain trilinear decomposition of $\hat{\mathcal{R}}$ via the COMFAC algorithm, thus obtain the estimates of $\mathbf{A}_t$ and $\mathbf{A}_r$.
4	Construct $\mathbf{P}_t$ and $\mathbf{P}_r$ according to Eq.(23), and then get the DODs and DOAs via Eq.(24) and Eq.(25).

IV. ALGORITHM ANALYSIS AND CRB
A. IDENTIFIABILITY
Uniqueness is an important feature of PARAFAC analysis, which can be described as follows.

Theorem 1 [16]: For any PARAFAC decomposition model in (3), if the factor matrices $\left\{\mathbf{A}^{(n)}\right\}_{n=1}^{N}$ are full k-rank. Once

$$\sum_{n=1}^{N} k_{\mathbf{A}^{(n)}} \geq 2K + 2 \qquad (33)$$

then $\left\{\mathbf{A}^{(n)}\right\}_{n=1}^{N}$ are unique up to permutation and scaling of columns, where $k_{\mathbf{A}^{(n)}}$ represents the k-rank of $\mathbf{A}^{(n)}$.

Theorem 1: reveals the identifiability of the proposed algorithm. In combination with (21) one can observe that the proposed algorithm can identify $\frac{M+N+MN-2}{2}$ at most. in Table 3, we summarize the identifiability of our algorithm, ESPRIT [10], HOSVD and its covariance version [17] (marked with C-HOSVD), PARAFAC [18] as well as QALS [32]. To make a fair comparison with ESPRIT, the HOSVD and C-HOSVD in the following are equal to HOSDV-ESPRIT and C-HOSVD-ESPRIT, respectively, i.e., after the subspace have been obtained by HOSVD and C-HOSVD, the ESPRIT-like technique is adopted to obtain the DODs and DOAs. It is shown that the proposed estimator has lower identifiability than the subspace methods (e.g., ESPRIT, HOSVD and C-HOSVD), while it can identify more targets than PARAFAC and QALS when $MN > M+N$.

TABLE 3. Comparisons of various algorithms.

Method	Identifiability	Flexibility	Complexity
ESPRIT	$\min\{MN-M, MN-N\}$	low	low
HOSVD	$\min\{MN-M, MN-N\}$	low	high
C-HOSVD	$\min\{MN-M, MN-N\}$	hige	high
PARAFAC	$M+N-2$	medium	medium
QALS	$M+N-1$	high	high
Proposed	$(M+N+MN-2)/2$	high	medium

B. FLEXIBILITY AND COMPLEXITY
ESPRIT is only suitable for uniform linear array (ULA). The HOSVD and C-HOSVD can work with arbitrary linear geometry by replacing ESPRIT with MUSIC. From Eq. (23) and Eq. (24) one can find that the proposed algorithm is for arbitrary linear manifolds (and even arbitrary manifolds, interested readers are recommend to refer [23] for more details), and so deos the QALS method. The flexibility of the proposed estimator is verified via simulation. We provide the scatter results of the proposed estimator in Figure 2, where $M = 4$, $N = 5$ and SNR=10 (the defination of the parameters can be find in the simulation section, other paramters are the same to that in *Examle 1*), $\left[d_{t,1}, d_{t,2}, d_{t,3}\right]^T = [0.45, 0.75, 1.00]^T$, $\left[d_{r,1}, d_{r,2}, d_{r,3}, d_{r,4}\right]^T = [0.40, 0.85, 1.15, 1.90]^T$. It is seen that the DODs and DOAs can be correct estimated and paired. Moreover, the covariance-based frameworks, i.e., C-HOSVD, QALS and the proposed algorithm, can be
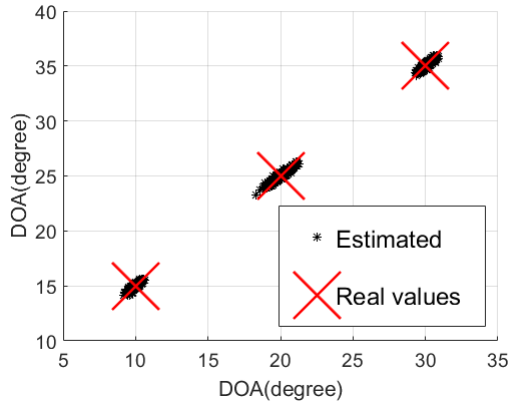
FIGURE 2. Scatter results of the proposed estimator with nonuniform arrays.

easily extended to spatially colored noise scenario. In summary, C-HOSVD, QALS and the proposed algorithm are more flexible than the others.

It is usually very hard to count the detailed calculation of each algorithm. In this paper, we only make an approximate estimation on the dominant burden of each algorithm. The main complexity of the above mentioned subspace methods is eigendecomposition, therefore, the complexity of all the algorithms are analized in terms of the eigendecomposition. For a $m \times n$ matrix, the SVD needs $O\left(mn^2\right)$ complex multiplication [41]. Therefore, the complexity of ESPRIT is on the order $O\left(M^3N^3\right)$. The eigdecomposition in HOSVD and C-HOSVD are on the order $O\left(MNL^2 + MN^2L + M^2NL\right)$ and $O\left(2M^3N^4 + 2M^4N^3\right)$, respectively. In QALS, the inilizations are obtained via traditional algorithm(e.g., MUSIC, ESPRIT, PM), and the ALS fittings are conducted in original space, making it is computationally much complex than ESPRIT and HOSVD. Moreover, for nonuniform array geometries, spectrum grid search in both methods require extra calculations, hence HOSVD, C-HOSVD and QALS are computationally costly. In PARAFAC and the proposed algorithm, the truncated SVD need $O\left(MK^2 + NK^2 + LK^2\right)$ and $O\left(MK^2 + NK^2 + MNK^2\right)$, respectively. From this point of view, the proposed algorithm is computationally attractive, espectively with large snapshot L or massive MIMO configuration. Also, the flexibility and complexity of various algorithm have been summarized in Table 1.

C. STOCHASTIC CRB

Refer to [42], we have derived the stochastic CRB on joint DOD and DOA estimation with unknown spatially colored noise field [43]. Let $\mathbf{R}_n = \mathbf{Q}(\mathbf{q})$, where $\mathbf{q} = [q_1, q_2, \cdots, q_P]^T$ is a real vector to parameterize the noise covariance. The stochastic CRB is given by

$$\text{CRB}(\theta, \varphi) = \frac{1}{L} \left[\mathbf{H} - \mathbf{M}\mathbf{T}^{-1}\mathbf{M}^T \right]^{-1} \quad (34)$$

with

$$\begin{cases} \mathbf{H} = 2\text{Re}\left\{ \left(\tilde{\mathbf{D}}^H \Pi_{\tilde{\mathbf{A}}}^{\perp} \tilde{\mathbf{D}}\right) \oplus \left(\left(\mathbf{R}_b \tilde{\mathbf{A}}^H \tilde{\mathbf{R}}_y^{-1} \tilde{\mathbf{A}} \mathbf{R}_b\right) \otimes \mathbf{1}_{2 \times 2}\right) \right\} \\ \mathbf{M} = 2\text{Re}\left\{ \begin{bmatrix} \mathbf{J}^T \left(\left(\tilde{\mathbf{D}}_{\theta}^H \Pi_{\tilde{\mathbf{A}}}^{\perp}\right) \otimes \left(\tilde{\mathbf{R}}^{-1} \tilde{\mathbf{A}} \mathbf{R}_b\right)^T \right) \tilde{\mathbf{Q}}^* \\ \mathbf{J}^T \left(\left(\tilde{\mathbf{D}}_{\varphi}^H \Pi_{\tilde{\mathbf{A}}}^{\perp}\right) \otimes \left(\tilde{\mathbf{R}}^{-1} \tilde{\mathbf{A}} \mathbf{R}_b\right)^T \right) \tilde{\mathbf{Q}}^* \end{bmatrix} \right\} \\ \mathbf{T} = 2\text{Re}\left\{ \tilde{\mathbf{Q}}^H \left(\tilde{\mathbf{R}}^{-T} \otimes \Pi_{\tilde{\mathbf{A}}}^{\perp}\right) \tilde{\mathbf{Q}} \right\} - \tilde{\mathbf{Q}}^H \left(\left(\Pi_{\tilde{\mathbf{A}}}^{\perp}\right)^T \otimes \Pi_{\tilde{\mathbf{A}}}^{\perp} \right) \tilde{\mathbf{Q}} \end{cases}$$

$$(35)$$

where $\oplus$ denotes the Hadamard product. $\tilde{\mathbf{A}} = \mathbf{Q}^{-1/2}\mathbf{A}$, $\Pi_{\tilde{\mathbf{A}}}^{\perp} = \mathbf{I} - \Pi_{\tilde{\mathbf{A}}}$ with $\Pi_{\tilde{\mathbf{A}}} = \tilde{\mathbf{A}}\tilde{\mathbf{A}}^{\dagger}$. $\tilde{\mathbf{D}} = \left[\tilde{\mathbf{D}}_{\theta}, \tilde{\mathbf{D}}_{\varphi} \right]$, $\tilde{\mathbf{D}}_{\theta} = \mathbf{Q}^{-1/2}\mathbf{D}_{\theta}$ and $\tilde{\mathbf{D}}_{\varphi} = \mathbf{Q}^{-1/2}\mathbf{D}_{\varphi}$ with $\mathbf{D}_{\theta} = \left[\mathbf{a}_t(\varphi_1) \otimes \frac{\partial \mathbf{a}_r(\theta_1)}{\partial \theta_1}, \cdots, \mathbf{a}_t(\varphi_K) \otimes \frac{\partial \mathbf{a}_r(\theta_K)}{\partial \theta_1}, \right]$ and $\mathbf{D}_{\varphi} = \left[\frac{\partial \mathbf{a}_t(\varphi_1)}{\partial \varphi_1} \otimes \mathbf{a}_r(\theta_1), \cdots, \frac{\partial \mathbf{a}_t(\varphi_K)}{\partial \varphi_K} \otimes \mathbf{a}_r(\theta_K) \right]$, respectively. $\tilde{\mathbf{R}}_y = \mathbf{Q}^{-1/2}\mathbf{R}_y\mathbf{Q}^{-1/2}$, $\mathbf{1}_{2 \times 2}$ is a 2×2 matrix filled with ones. $\mathbf{J} = \left[\text{vec}\left\{ \mathbf{e}_1 \mathbf{e}_1^T \right\}, \text{vec}\left\{ \mathbf{e}_2 \mathbf{e}_2^T \right\}, \cdots, \text{vec}\left\{ \mathbf{e}_K \mathbf{e}_1^T \right\} \right]$, with $\mathbf{e}_k$ denotes the k-th column of the $K \times K$ identity matrix, $\text{vec}\{\cdot\}$ denotes the vectorization operation. $\tilde{\mathbf{Q}} = \left[\text{vec}\left\{ \tilde{\mathbf{Q}}_1' \right\}, \text{vec}\left\{ \tilde{\mathbf{Q}}_2' \right\}, \cdots, \text{vec}\left\{ \tilde{\mathbf{Q}}_P' \right\} \right]$ with $\tilde{\mathbf{Q}}_p' = \mathbf{Q}^{-1/2}\mathbf{Q}_p'\mathbf{Q}^{-1/2}$, $\tilde{\mathbf{Q}}_p' = \frac{\partial \mathbf{Q}}{\partial q_p}$.

V. SIMULATION RESULTS

In this section, the superiority of the covariance-based trilinear decomposition estimator is verified via Monte Carlo simulation. We consider a bistatic scenario, where the MIMO radar configured with M transmit antenna and N receive antenna. For fair comparison with the existing rotation invariance technique-based solutions, both the transmitters and the receivers are assumed to be ULAs with inter-element distance is half-wavelength. Suppose $K = 3$ uncorrelated sources located at the angles $(\theta_1, \varphi_1) = (10°, 15°), (\theta_2, \varphi_2) = (20°, 25°), (\theta_1, \varphi_1) = (30°, 35°)$, and Doppler frequencies are $\{f_k\}_{k=1}^3 = \{200, 400, 850\}$Hz, respectively. The reflection coefficients $\beta_{k,\tau}$ are randomly generated, the sampling frequency is $f_s = 2$KHz and L snapshots are collected. In this paper, the matched filtering processing is ignored. All the simulation results are relay on the data model in Eq. (10). The signal-to-noise ratio (SNR) in the simulation is defined as $\text{SNR} = 10\log_{10}\|\mathbf{Y}_s - \mathbf{N}_s\|^2 / \|\mathbf{N}_s\|^2$ [dB], where $\mathbf{Y}_s$ and $\mathbf{N}_s$ are the matrices given in (13). Two scenarios have been considered in the simulation, **I**) Gaussian white noise case, **II**) spatially colored noise case with the (m, n)-th element of $\mathbf{C}$ is $\mathbf{C}(m, n) = \alpha \cdot \exp\{-|m - n|\beta\}$, where β is the noise 'colored' parameter. All the curves are based on 500 independent trials. To evaluate the estimation performance, two metrics are adopted. One is the root mean square error (RMSE), which is defined as

$$\text{RMSE} = \frac{1}{K}\sum_{k=1}^K \sqrt{\frac{1}{500}\sum_{i=1}^{500} \left\{ \left(\hat{\theta}_{i,k} - \theta_k\right)^2 + \left(\hat{\varphi}_{i,k} - \varphi_k\right)^2 \right\}}$$

where $\hat{\theta}_{i,k}$ and $\hat{\varphi}_{i,k}$ are the estimates of θ_k and φ_k in the i th trial. The other one is the probability of the successful

detection (PSD). When the absolute error of all the estimated angles in a trial are smaller than 0.3°, it will be recorded to calculate the PSD.

Example 1: The estimation performance of the proposed estimator is tested at various SNR value, where $M = 8$, $N = 8$, $L = 500$ and scenario **I** are considered. For comparison, the performance ESPRIT [10], HOSVD [17], C-HOSVD [17] in both HOSVD and C-HOSVD, the ESPRIT technique is adopted once the signal subspace is obtained, thus no step searching is required, PARAFAC [18] as well as QALS [32] (initialized by PM) are added. It is shown in Figure 3 that QALS would fail to work at low SNR regions, owing to imprecise initializations. Moreover, the proposed algorithm has very close RMSE with PARAFAC, both of which provide lower RMSE than the other methods. Notably, all the methods exhibit a 100% PSD at high SNR regions. With the decreasing SNR, the PSD of each algorithm starts to drop at a certain point, which is known as the SNR threshold [31]. One can observe that both PARAFAC and the proposed method have lower SNR thresholds than the other methods, as depicted in Figure 4. The improvements benefit from two aspects. On the one hand, the iterative strategy in COMFAC help to achieve more accurate direction matrices. On the other hand, the LS fitting in angle estimation can make full use of the array apertures.

FIGURE 4. PSD versus SNR in scenario I.

FIGURE 5. RMSE versus L in scenario I.

FIGURE 3. RMSE versus SNR in scenario I.

Example 2: We compare the estimation performance with different snapshot L in scenario **I**, where $M = N = 8$ and SNR is fixed at 0dB. Figure 5 and Figure 6 illustrate the performance curves. As expected, PARAFAC, QALS and the proposed algorithms provide lower RMSE and offer lower L thresholds than the other methods. Also, one can see that QALS may fail to work with small snapshot.

Example 3: We repeat *Example* 1 but now scenario **II** is considered, with $\alpha = 0.9$ and $\beta = 0.1$. For comparison, the performance of temporal cross-correlation based ESPRIT algorithm in [30] (marked with T-ESPRIT), the spatial cross-correlation based HOSVD algorithm in [29]
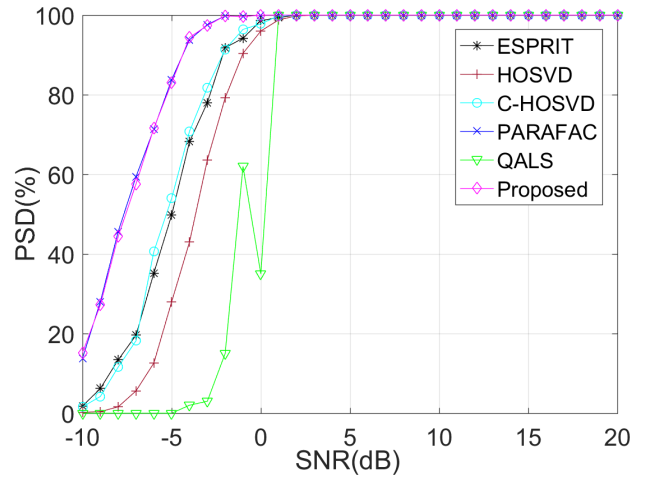

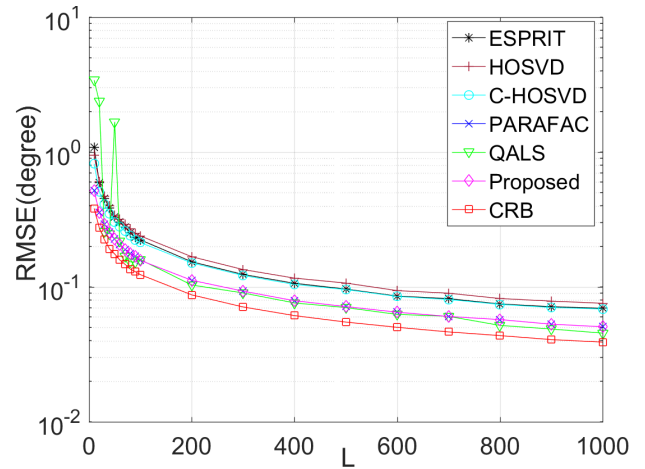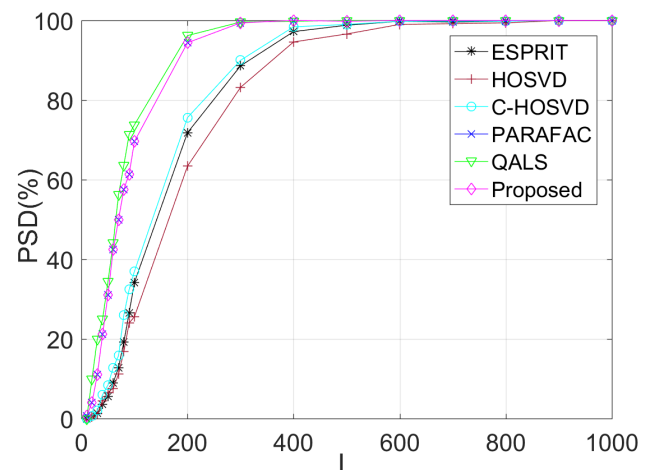**FIGURE 6.** PSD versus L in scenario I.

(marked with S-HOSVD), the PARAFAC method in [18] and the temporal cross-correlation based QALS algorithm in [32] (marked with T-QALS) are added. Figure 7 and Figure 8
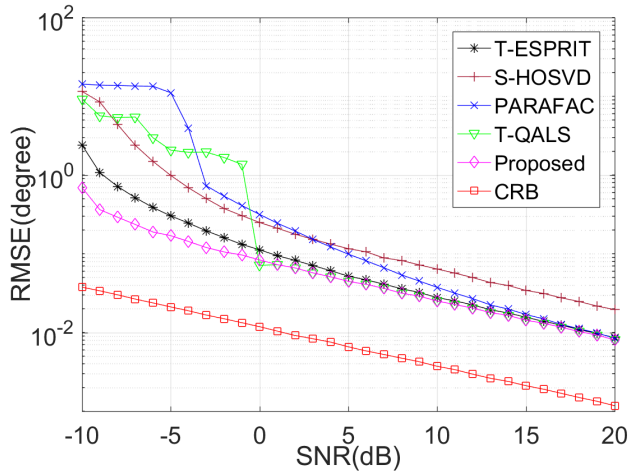
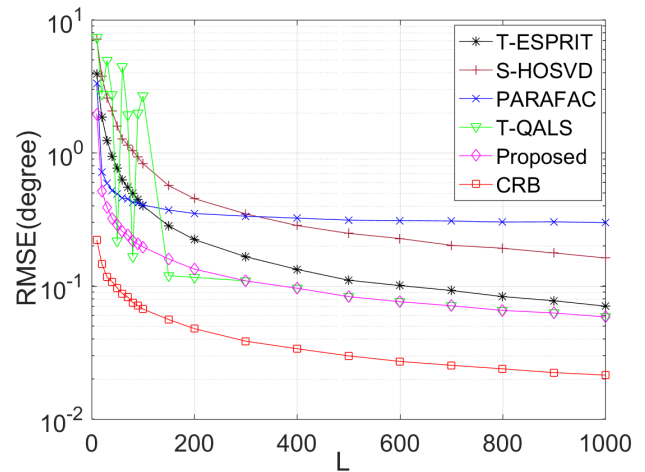**FIGURE 7.** RMSE versus SNR in scenario **II**.
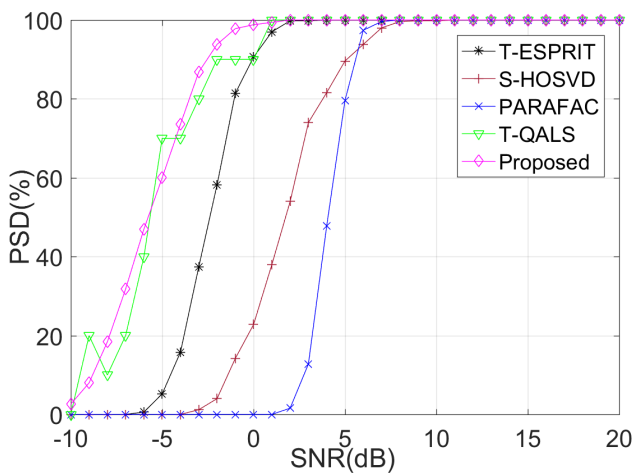

FIGURE 9. RMSE versus L in scenario **II**.

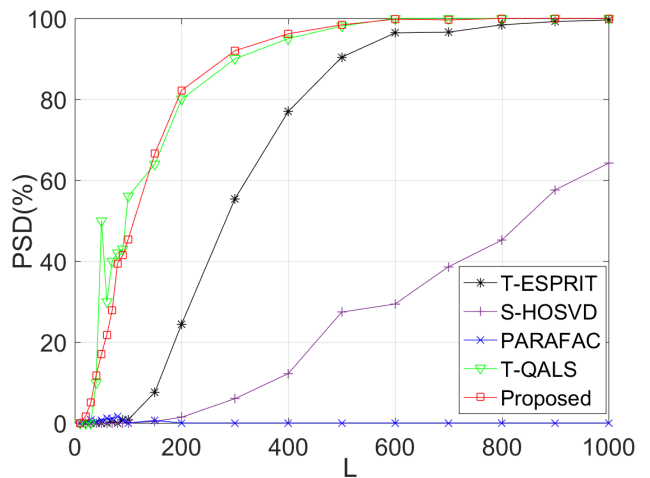**FIGURE 8.** PSD versus SNR in scenario **II**.

FIGURE 10. PSD versus L in scenario **II**.

give the results. Certainly, the traditional PARAFAC method fails to work at low SNR regions, neither does T-QALS can properly work. An interesting observation is that the proposed algorithm outperform all the compared methods, corroborating the flexibility of our algorithm.

Example 4: We repeat *Example* 2 in scenario **II**, where α and β are fixed at 0.9 and 0.1, respectively. Figure 9 and Figure 10 present the performance curves. Similarly, the proposed algorithm has lower RMSE at low L regions, and it offers very close RMSE performance to T-QALS when L≥300. Furthermore, it provides much lower L thresholds than T-ESPRIT, S-HOSVD and PARAFAC. As shown in Figure 9, the RMSE of the PARAFAC algorithm is larger than 0.3°, thus it provides a 0% PSD. It is evident that the proposed algorithm is valid for spatially colored noise scenario.

Example 5: The performance of various methods with different 'colored' parameter β is examined, where $M = N = 8$, $L = 500$, $\alpha = 0.9$ and SNR=0dB, respectively. Figure 11 and Figure 12 display the results. Worthnoting is that $\mathbf{C} \approx \alpha\mathbf{I}$

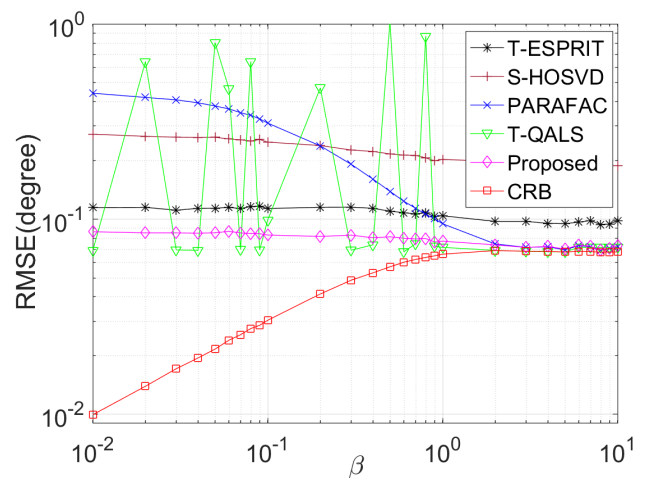**FIGURE 11.** RMSE versus β in scenario **II**.

when $\beta \gg 1$. It is shown that PARAFAC is sensitive to β. The performance of other algorithms barely change since they are suitable for colored noise scenario, while RMSE of QALS is not stable in such example.
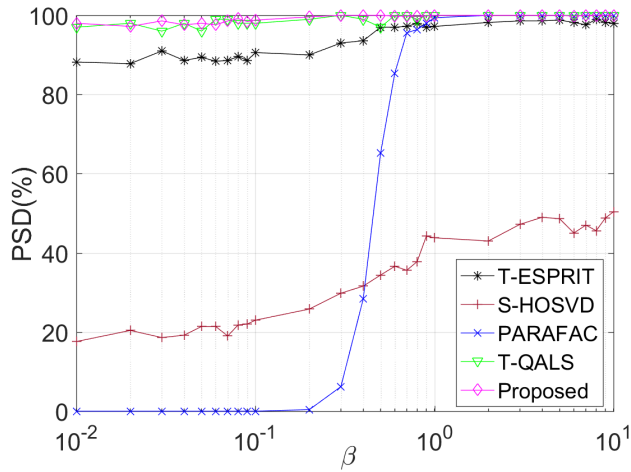
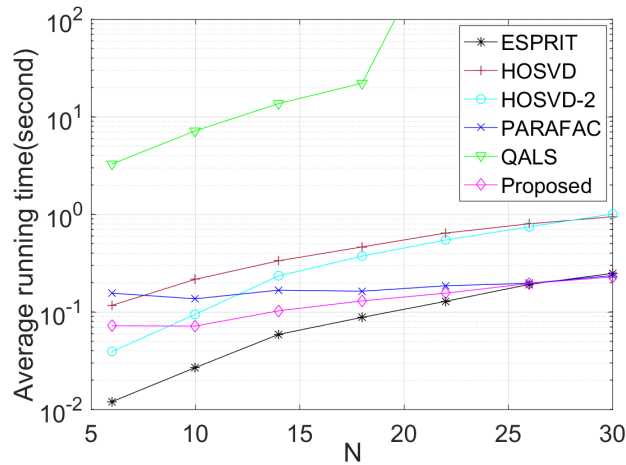**FIGURE 12.** PSD versus β in scenario II.

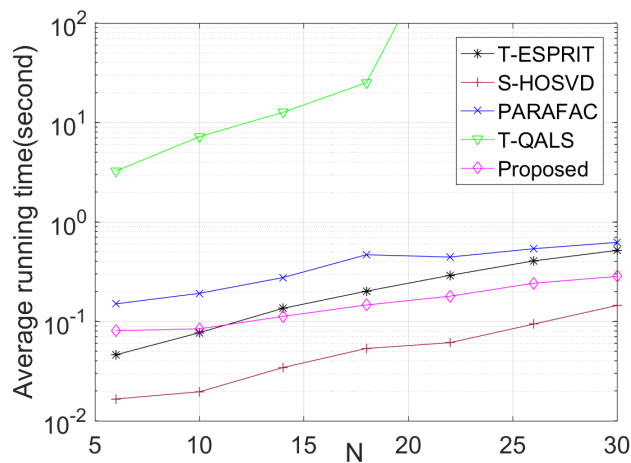**FIGURE 13.** Average running time versus N in scenario I.

FIGURE 14. Average running time versus N in scenario II.

Example 6: We compare the average running time in terms of receive antenna number N in both scenarios, where $M = 32$, $L = 1000$, SNR$= -5$dB are considered. As depicted in Figure 13 and Figure 14, for each algorithm,

more intensive computations are required with the increasing N. Beside, the proposed algorithm is more efficient than the HOSVD-based methods in scenario I, and it is less complex than ESPRIT and PARAFAC in scenario II. Most importantly, the complexity of our algorithm is improved by two or three orders of magnitude in contrast to the QALS method.

VI. CONCLUSION

In this paper, we address the direction finding problem in bistatic MIMO radar. A covariance-based trilinear decomposition algorithm is presented, which makes full use of the tensor nature of the array measurement form the covariance perspective, and it can be easily extended to the spatially colored noise scenario. From an engineering point of view, the proposed scheme has reached a good compromise between accuracy and efficiency. The proposed covariance-based trilinear decomposition algorithm should also be of interest in other areas.

REFERENCES

[1] E. Fishler, A. Haimovich, R. Blum, D. Chizhik, L. Cimini, and R. Valenzuela, "MIMO radar: An idea whose time has come," in *Proc. IEEE Radar Conf.*, Philadelphia, PA, USA, Apr. 2004, pp. 71–78.

[2] P. Stoica, J. Li, and Y. Xie, "On probing signal design for MIMO radar," *IEEE Trans. Signal Process.*, vol. 55, no. 8, pp. 4151–4161, Aug. 2007.

[3] J. Li, P. Stoica, L. Xu, and W. Roberts, "On parameter identifiability of MIMO radar," *IEEE Signal Process. Lett.*, vol. 14, no. 12, pp. 968–971, Dec. 2007.

[4] A. Haimovich, R. Blum, and L. Cimini, "MIMO radar with widely separated antennas," *IEEE Signal Process. Mag.*, vol. 25, no. 1, pp. 116–129, Dec. 2008.

[5] J. Li and P. Stoica, "MIMO radar with colocated antennas," *IEEE Signal Process. Mag.*, vol. 24, no. 5, pp. 106–114, Sep. 2007.

[6] I. Bekkerman and J. Tabrikian, "Target detection and localization using MIMO radars and sonars," *IEEE Trans. Signal Process.*, vol. 54, no. 10, pp. 3873–3883, Oct. 2006.

[7] H. Yan, J. Li, and G. Liao, "Multitarget identification and localization using bistatic MIMO radar systems," *EURASIP J. Adv. Signal Process.*, vol. 2008, Jan. 2008, Art. no. 283483.

[8] F. Wen, "Computationally efficient DOA estimation algorithm for MIMO radar with imperfect waveforms," *IEEE Commun. Lett.*, vol. 23, no. 6. doi: 10.1109/LCOMM.2019.2911285.

[9] Z. D. Zheng and J. Y. Zhang, "Fast method for multi-target localisation in bistatic MIMO radar," *Electron. Lett.*, vol. 47, no. 2, pp. 138–139, Jan. 2011.

[10] C. Duofang, C. Baixiao, and Q. Guodong, "Angle estimation using ESPRIT in MIMO radar," *Electron. Lett.*, vol. 44, no. 12, pp. 770–771, Jun. 2008.

[11] X. Wang, W. Wang, J. Liu, X. Li, and J. Wang, "A sparse representation scheme for angle estimation in monostatic MIMO radar," *Signal Process.*, vol. 104, no. 6, pp. 258–263, Nov. 2014.

[12] J. Liu, X. Wang, and W. Zhou, "Covariance vector sparsity-aware DOA estimation for monostatic MIMO radar with unknown mutual coupling," *Signal Process.*, vol. 119, pp. 21–27, Feb. 2016.

[13] D. Nion and N. D. Sidiropoulos, "Tensor algebra and multidimensional harmonic retrieval in signal processing for MIMO radar," *IEEE Trans. Signal Process.*, vol. 58, no. 11, pp. 5693–5705, Nov. 2010.

[14] T. G. Kolda and B. W. Bader, "Tensor decompositions and applications," *SIAM Rev.*, vol. 51, no. 3, pp. 455–500, Aug. 2009.

[15] M. Haardt, F. Roemer, and G. D. Galdo, "Higher-order SVD-based subspace estimation to improve the parameter estimation accuracy in multidimensional harmonic retrieval problems," *IEEE Trans. Signal Process.*, vol. 56, no. 7, pp. 3198–3213, Jul. 2008.

[16] T. Jiang and N. D. Sidiropoulos, "Kruskal's permutation lemma and the identification of CANDECOMP/PARAFAC and bilinear models with constant modulus constraints," *IEEE Trans. Signal Process.*, vol. 52, no. 9, pp. 2625–2636, Sep. 2004.

[17] Y. Cheng, R. Yu, H. Gu, and W. Su, "Multi-SVD based subspace estimation to improve angle estimation accuracy in bistatic MIMO radar," *Signal Process.*, vol. 93, no. 7, pp. 2003–2009, Jul. 2013.

[18] X. Zhang, Z. Xu, L. Xu, and D. Xu, "Trilinear decomposition-based transmit angle and receive angle estimation for multiple-input multiple-output radar," *IET Radar Sonar Navigat.*, vol. 5, no. 6, pp. 626–631, Jul. 2011.

[19] J. Li and M. Zhou, "Improved trilinear decomposition-based method for angle estimation in multiple-input multiple-output radar," *IET Radar, Sonar Navigat.*, vol. 7, no. 9, pp. 1019–1026, Dec. 2013.

[20] B. Xu, Y. Zhao, Z. Cheng, and H. Li, "A novel unitary PARAFAC method for DOD and DOA estimation in bistatic MIMO radar," *Signal Process.*, vol. 138, pp. 273–279, Sep. 2017.

[21] X. Wang, W. Wang, J. Liu, Q. Liu, and B. Wang, "Tensor-based real-valued subspace approach for angle estimation in bistatic MIMO radar with unknown mutual coupling," *Signal Process.*, vol. 116, pp. 152–158, Nov. 2015.

[22] J. Li, X. Zhang, and X. Gao, "A joint scheme for angle and array gain-phase error estimation in bistatic MIMO Radar," *IEEE Geosci. Remote Sens. Lett.*, vol. 10, no. 6, pp. 1478–1482, Nov. 2013.

[23] J. Li and X. Zhang, "A method for joint angle and array gain-phase error estimation in bistatic multiple-input multiple-output non-linear arrays," *IET Signal Process.*, vol. 8, no. 2, pp. 131–137, Apr. 2014.

[24] F. Wen, X. Xiong, and Z. Zhang, "Angle and mutual coupling estimation in bistatic MIMO radar based on PARAFAC decomposition," *Digit. Signal Process.*, vol. 65, pp. 1–10, Jun. 2017.

[25] F. Wen, Z. Zhang, K. Wang, G. Sheng, and G. Zhang, "Angle estimation and mutual coupling self-calibration for ULA-based bistatic MIMO radar," *Signal Process.*, vol. 144, pp. 61–67, Mar. 2018.

[26] M. Jin, G. Liao, and J. Li, "Joint DOD and DOA estimation for bistatic MIMO radar," *Signal Process.*, vol. 89, no. 2, pp. 244–251, Feb. 2009.

[27] J. Chen, H. Gu, and W. Su, "A new method for joint DOD and DOA estimation in bistatic MIMO radar," *Signal Process.*, vol. 90, no. 2, pp. 714–718, Feb. 2010.

[28] H. Jiang, J.-K. Zhang, and K. M. Wong, "Joint DOD and DOA estimation for bistatic MIMO radar in unknown correlated noise," *IEEE Trans. Veh. Technol.*, vol. 64, no. 11, pp. 5113–5125, Nov. 2015.

[29] X. Wang, W. Wang, X. Li, and J. Wang, "A tensor-based subspace approach for bistatic MIMO radar in spatial colored noise," *Sensors*, vol. 14, no. 3, pp. 3897–3907, Feb. 2014.

[30] W.-B. Fu, T. Z. Su, Y.-B. Zhao, and X.-H. He, "Joint estimation of angle and doppler frequency for bistatic MIMO radar in spatial colored noise based on temporal-spatial structure," *J. Electron. Inf. Technol.*, vol. 33, no. 7, pp. 1649–1654, Jul. 2011.

[31] F. Wen, X. Xiong, J. Su, and Z. Zhang, "Angle estimation for bistatic MIMO radar in the presence of spatial colored noise," *Signal Process.*, vol. 134, pp. 261–267, May 2017.

[32] Z. Wang, C. Cai, F. Wen, and D. Huang, "A quadrilinear decomposition method for direction estimation in bistatic MIMO radar," *IEEE Access*, vol. 6, pp. 13766–13772, 2018.

[33] S. Hong, X. Wan, F. Cheng, and H. Ke, "Covariance differencing-based matrix decomposition for coherent sources localisation in bi-static multiple-input–multiple-output radar," *IET Radar Sonar Navigat.*, vol. 9, no. 5, pp. 540–549, Jun. 2015.

[34] F. Wen, Z. Zhang, G. Zhang, Y. Zhang, X. Wang, and X. Zhangc, "A tensor-based covariance differencing method for direction estimation in bistatic MIMO radar with unknown spatial colored noise," *IEEE Access*, vol. 5, pp. 18451–18458, 2017.

[35] H. Huang, J. Yang, Y. Song, H. Huang, and G. Gui, "Deep learning for super-resolution channel estimation and DOA estimation based massive MIMO system," *IEEE Trans. Veh. Technol.*, vol. 67, no. 9, pp. 8549–8560, Sep. 2018.

[36] H. Huang, Y. Song, J. Yang, G. Gui, and F. Adachi, "Deep-learning-based millimeter-wave massive MIMO for hybrid precoding," *IEEE Trans. Veh. Technol.*, vol. 68, no. 3, pp. 3027–3032, Mar. 2019.

[37] W. Rao, D. Li, and J. Q. Zhang, "A tensor-based approach to L-shaped arrays processing with enhanced degrees of freedom," *IEEE Signal Process. Lett.*, vol. 25, no. 2, pp. 1–5, Feb. 2018.

[38] B. Liao, "Fast angle estimation for MIMO radar with nonorthogonal waveforms," *IEEE Trans. Aerosp. Electron. Syst.*, vol. 54, no. 4, pp. 2091–2096, Aug. 2018.

[39] S. A. Vorobyov, Y. Rong, N. D. Sidiropoulos, and A. B. Gershman, "Robust iterative fitting of multilinear models," *IEEE Trans. Signal Process.*, vol. 53, no. 8, pp. 2678–2689, Aug. 2005.

[40] R. Bro, N. Sidiropoulos, and G. Giannakis, "A fast least squares algorithm for separating trilinear mixtures," in *Proc. Int. Workshop Independ. Compon. Blind Signal Separat. Anal*, Jan. 1999, pp. 11–15.

[41] B. I. D. N. Lloyd Trefethen, *Numerical Linear Algebra*. Philadelphia: Society for Industrial and Applied Mathematics, 1997.

[42] A. B. Gershman, P. Stoica, M. Pesavento, and E. G. Larsson, "Stochastic Cramér–Rao bound for direction estimation in unknown noise fields," *IET Radar, Sonar Navigat.*, vol. 149, no. 1, pp. 2–8, Feb. 2002.

[43] F. Wen, Z. Zhang, and X. Zhang, "CRBs for direction-of-departure and direction-of-arrival estimation in collocated MIMO radar in the presence of unknown spatially coloured noise," *IET Radar, Sonar Navigat.*, vol. 13, no. 4, pp. 530–537, Apr. 2019.

FANGQING WEN was born in Hubei, China, 1988. He received the B.S. degree in electronic engineering from the Hubei University of Automotive Technology, Shiyan, China, in 2011, and the master's and Ph.D. degrees from the College of Electronics and Information Engineering, Nanjing University of Aeronautics and Astronautics (NUAA), China, in 2013 and 2016, respectively. From 2015 to 2016, he was a Visiting Scholar with the University of Delaware, USA. Since 2016, he has been with the Electronic and Information School, Yangtze University, China, where he is currently an Assistant Professor. His research interests include MIMO radar, array signal processing, and compressive sensing. He is a member of the Chinese Institute of Electronics (CIE). He is an Associate Editor of the journal *Electronics Letters*.

ZIJING ZHANG was born in Beijing, China, in 1967. He received the B.S. and M.S. degrees in dynamics from the Harbin Institute of Technology, Harbin, China, in 1989 and 1992, respectively, and the Ph.D. degree in electrical engineering from Xidian University, Xi'an, China, in 2001. In 2006, he was a Visiting Scholar with the University of Manchester, U.K. In 2016, he was a Visiting Scholar with the University of Delaware, USA. Since 1992, he has been with the National Laboratory of Radar Signal Processing, Xidian University. His current research interests include radar signal processing and multirate filter banks design.

GONG ZHANG received the Ph.D. degree in electronic engineering from NUAA, Nanjing, China, in 2002. From 1990 to 1998, he was a Member of Technical Staff with No724 Institute China Shipbuilding Industry Corporation (CSIC), Nanjing. Since 1998, he has been with the College of Electronics and Information Engineering, NUAA, where he is currently a Professor. His research interests include radar signal processing and compressive sensing. He is a member of the Committee of Electromagnetic Information and the Chinese Society of Astronautics (CEI-CSA), and a Senior Member of the Chinese Institute of Electronics (CIE).

• • •